



RESEARCH ARTICLE

10.1002/2016RS006232

Key Points:

- The ionospheric channel is studied in terms of frequency availability and time
- Comparison among the ITU Rec533 prediction, the OIS availability and the VIS MUF values on the path
- OIS availability estimation in function of VIS sounding results

Correspondence to:

R. M. Alsina-Pagès,
ralsina@salleurl.edu

Citation:

Alsina-Pagès, R. M., M. Hervás, D. Altadill, J. Calduch, and E. Blanch (2017), Vertical and oblique ionospheric soundings performance comparison over the 12,760 km transequatorial HF link between Antarctica and Spain, *Radio Sci.*, 52, 498–510, doi:10.1002/2016RS006232.


Received 10 DEC 2016

Accepted 29 MAR 2017

Accepted article online 10 APR 2017

Published online 29 APR 2017

Vertical and oblique ionospheric soundings performance comparison over the 12,760 km transequatorial HF link between Antarctica and Spain

R. M. Alsina-Pagès¹ , M. Hervás¹ , D. Altadill² , J. Calduch¹, and E. Blanch² 

¹GTM-Grup de recerca en Tecnologies Mèdia, La Salle-Universitat Ramon Llull, Barcelona, Spain, ²Observatori de l'Ebre, CSIC-Universitat Ramon Llull, Roquetes, Spain

Abstract This paper presents the second part of the study of the oblique sounding of a 12,760 km transequatorial ionospheric link between Livingston Island (Antarctica) and Cambrils in Spain. The study consists of the comparison among the oblique sounding results using an inverted V as receiver antenna, the International Telecommunication Union Rec533 HF prediction model, and the vertical sounding results on the path of the long haul channel. The data were collected the last consecutive surveys, when the inverted V antenna was operative (2010–2011, 2011–2012, 2012–2013, and 2013–2014). The ionospheric channel is studied in terms of frequency availability depending on time using the measurements of an oblique incidence sounder (OIS) and also measurements of several vertical incidence sounding stations (VIS) on the path of the long haul channel. The results obtained show similarities between the VIS and the OIS measurements; following previous studies preliminary results, the experiments conducted led us to think that the frequency of large availability can be estimated depending on the VIS sounding results.

1. Introduction

La Salle has been involved for 11 years in a project which goal is to design a high frequency (HF) transequatorial radio link from the Spanish Antarctic Station (SAS) in Livingston Island (62.6°S, 60.4°W) to Cambrils, in Spain (41.0°N, 1.0°E) [Pijoan *et al.*, 2014; Alsina-Pagès *et al.*, 2016]. The main objectives of this study are to implement a long haul oblique ionospheric sounder and to transmit data from sensors located at the SAS to Cambrils. The distance between transmitter and receiver is of 12,760 km, so around four hops of the wave propagation are expected [Perkiomaki, 2013], as we have detailed in previous studies [Ads *et al.*, 2015]. The propagation path is shown in Figure 1, where the estimated four hops are drawn as H_i , while the transmitter is labeled as SAS and the receiver as CB (Cambrils) (for more detailed information about the stations, the hops, and the distance in-between, see Tables 1 and 2).

Oblique soundings have been studied in the literature [Jackson-Booth *et al.*, 2012], most of them centered in one-hop analysis [Warrington *et al.*, 2000]. The frequency selection is a key issue for the HF modem design [Angling *et al.*, 1998]. The results of our oblique ionospheric sounding (OIS) have a complex interpretation in terms of ionospheric physics, because the link has four estimated hops and is transequatorial but are crucial in terms of channel propagation description for communications.

This work continues the study published by Ads *et al.* [2015]; in that work, we pretended to establish a prediction method for the frequency availability in the 12,700 km radio link between Livingston and the Ebro Observatory [Vilella *et al.*, 2008; Ads *et al.*, 2012]. Comparing the frequency availability of the transequatorial oblique incidence sounding (OIS) with the vertical incidence sounding (VIS) data, Ads *et al.* [2015] proved high correlation between OIS and VIS.

Other prediction environments can be found in the literature for midlatitude links [Shukla and Cannon, 1994] and for high latitudes [Jodalen *et al.*, 2001] for short links. However, Ads *et al.* [2015] showed for the first time that combining the measurements of VIS located along the transequatorial radio link path it is possible to estimate the frequency of large availability of the ionospheric channel. Ads *et al.* [2015] analyzed OIS measurements of the long haul transequatorial link 24 h a day comparing to six VIS stations (Port Stanley, Cachoeira Paulista, Fortaleza, Ascension Island, El Arenosillo, and Roquetes). The oblique incidence soundings were performed using a 7.5 m rugged monopole both in the transmitter and in the receiver for campaigns 2009–2010,

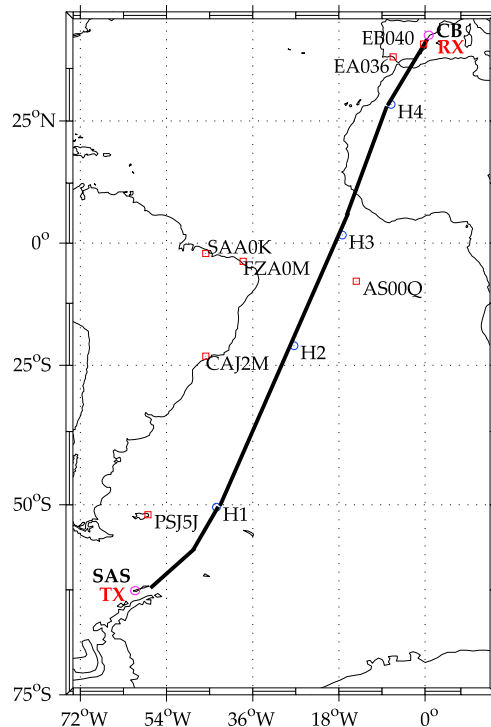


Figure 1. The locations of the VIS stations used in the study are indicated by their Union Radio Scientifique Internationale (URSI) codes and the four estimated hops of the radio link from the transmitter (Tx) in Spanish Antarctic Station (SAS) and the receiver (Rx) in Cambrils (CB) are indicated by H_i (for more details about the hop locations, the reader is referred to *Vilella et al.* [2009]).

2010–2011, and 2011–2012 [Ads et al., 2015]. The conclusions of the paper pointed out that the estimation of the frequency of largest availability (FLA) using the VIS stations information (Port Stanley, Cachoeira Paulista, Ascension Island, and El Arenosillo) showed promising results. Port Stanley station results were nearly not affecting the final frequency estimation.

In this paper we present the results for the last four campaigns using a 7.5 m rugged monopole in the transmitter (SAS) and an inverted V antenna in the receiver (CB). This changes the polarization reception in Spain (Cambrils), as well as the location of the receiver, and extends the study from 2010–2011 to 2013–2014, the four campaigns when the inverted V antenna has been operative in the new place. The inverted V antenna works with horizontal polarization, and the previously studied monopole works with vertical polarization. We have added Sao Luis VIS observatory to the five already studied stations due to the lack of data of Cachoeira

Table 1. The Location of the VIS Stations, the Reflection Hops, and the Equipment of the VIS Stations [Lowell Digisonde International, 2014]

Station	Latitude	Longitude	URSI Code	VIS Station Equipment
Port Stanley	51.7°S	57.8°W	PSJ5J	DPS1 Lowell Digisonde
H1	50.4°S	43.6°W		
Cachoeira Paulista	23.2°S	45.8°W	CAJ2 M	D256 Lowell Digisonde
Sao Luis	2.5°S	44.2°W	SAA0 K	D256 Lowell Digisonde
H2	23.1°S	27.4°W		
Fortaleza	3.7°S	38.8°W	FZA0 M	DPS4 Lowell Digisonde
Ascension Island	7.95°S	14.4°W	AS00Q	D256 Lowell Digisonde
H3	1.3°N	17.3°W		
El Arenosillo	37.1°N	6.7°W	EA036	D256 Lowell Digisonde
Roquetes (Ebro Observatory)	40.4°N	0.3°E	EB040	DPS4D Lowell Digisonde
H4	28.2°N	7.1°W		

Table 2. Distance (in km) Between the Ionospheric Stations in This Study and the Estimated Location of the Four Ionospheric Hops H_i

Stations/Hops	H1	H2	H3	H4
PSJ5J	960	4104	7010	10170
CAJ2 M	3031	1908	4115	7062
SAA0 K	5327	2754	3020	5229
FZA0 M	5212	2294	2453	4907
AS00Q	5435	2221	1078	4095
EA036	10380	6826	4127	990
EB040	10960	7415	4696	1516

Paulista and Fortaleza for some campaigns, and we have maintained Port Stanley despite its nearly negligible influence to the final results. We have also added Roquetes (Ebro Observatory) due to the lack of data of El Arenosillo, but we kept El Arenosillo while the data are available.

Our goal in this paper is to confirm the results of our work in *Ads et al.* [2015] with the comparison of more data and in a different channel impulse response due to the change of

antenna and location in the receiver. Moreover, we have studied the results for a different period of time: in *Ads et al.* [2015] the studied campaigns were 2009–2010, 2010–2011, and 2011–2012, and in this work we study 2010–2011, 2011–2012, 2012–2013, and 2013–2014 campaigns. Also important is to assess if the change of polarization at the receiver plays a role in the results of the FLA [Bergadà et al., 2016]. We compare the experimental OIS and VIS data with the estimated maximum usable frequency (MUF)(D) values [Perkiomaki, 2013], the maximum usable frequency obtained by the Rec533 for different levels of solar activity. The MUF(D) is defined as the highest frequency for which an ionospheric communication path is predicted on 50% of the days of the month [International Telecommunication Union-Recommendation, 2012]. These four surveys studied in this work have been conducted with the same range of transmission frequencies as in *Ads et al.* [2015] with the VIS and OIS systems also working 24 h a day. The communication availability of this remote system is often low due to the length of the channel; however, we analyze all the HF frequency range tested to assure we use the best frequency at each hour.

In section 2 we give details of the description of both sounding systems, OIS and VIS, its measurements, and the influence of the solar activity in the measurements. Section 3 presents the results of the time variation of $MUF(3000)F_2$, obtained from VIS, and the frequency of largest availability (FLA), obtained from OIS measurements. $MUF(3000)F_2$ is the maximum usable frequency for a single hop transmission at 3000 km reflected at the F_2 layer, which is measured from VIS ionograms. Section 4 compares the results of the time variation of the FLA with that of the $MUF(3000)F_2$. Finally, in section 5, the conclusions and the feasibility of frequency forecast are discussed.

2. Description of the Sounding System

In this section we introduce the OIS and the VIS systems, and the solar activity is briefly explained for the four consecutive surveys studied in this paper. In Table 3 the starting and ending date for the four campaigns are detailed, as well as the number of days that the system was operative.

2.1. Oblique Incidence Sounding

The oblique ionospheric sounder has been working since 2003, analyzing the channel using narrowband and wideband soundings, as well as with several wideband modulation tests, during the austral summer when the SAS is operative for research purposes. The receiver in Cambrils has three different antennas: a 7.5 m rugged monopole, an inverted V antenna, and a Yagui. For more details of the project and the receiver antenna, we refer the reader to Pijoan et al. [2014]. In this work we will analyze campaigns from 2010–2011 to 2013–2014

(a total of four campaigns), using the data received in Cambrils by the inverted V antenna. In *Ads et al.* [2015] the authors analyzed the campaigns 2009–2010 to 2011–2012, but using the monopole in the receiver. Unfortunately, only two campaigns have data available for both the monopole and the inverted V antenna.

Table 3. The Starting Date, the Final Date, and the Number of Days Per Survey for the Four Studied Campaigns

Survey	Starting Date	Final Date	No. of Days
2010/2011	22/1/2011	1/3/2011	39
2011/2012	13/2/2012	25/2/2012	13
2012/2013	5/1/2013	24/02/2013	51
2013/2014	24/1/2014	18/2/2014	26

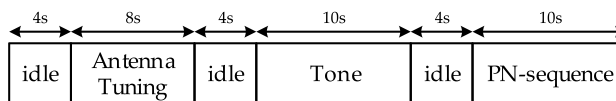


Figure 2. A sounding transmission frame structure, with the antenna tuning, the narrowband tone, and the wideband PN sequence transmission.

2.1.1. OIS Hardware Description

The last oblique ionospheric sounding system update was in 2009–2010 survey, and the new soundings were published by *Ads et al.* [2012]. The system today can operate in a range of [2, 30] MHz, 24 h a day and uses an oven controlled crystal oscillator (OCXO) and a GPS unit with a pulse per second signal that presents a time synchronization accuracy of 1 μ s. Both transmitter and receiver are based on software-defined radio (SDR) devices that are suitable to digitalize the entire HF band and work with high-speed analog to digital (ADC) and digital to analog (DAC) converters. The transmitter antenna is a 7.5 m rugged monopole, equipped with an antenna tuner that can adapt the whole HF band. The transmission power is limited to 250 W due to environmental and consumer power restrictions at the SAS. In the receiver, the inverted V antenna is used to feed the SDR platform that processes the signal. More details about the hardware can be found in *Alsina-Pagès et al.* [2016].

2.1.2. OIS Test Design

The transmitted signals are structured in a frame shown in Figure 2; they are conducted once every hour every day, using frequencies in the range of [2, 30] MHz in 0.5 MHz steps. First, the system adapts with the antenna tuning, then a full power tone is transmitted during 10 s to perform a narrowband sounding, and afterward a set of pseudo noise (PN) m sequences [Gold, 1968; Parsons, 2000] are sent to perform a 10 s wideband sounding [Proakis, 2000].

The narrowband tests are used to estimate the signal-to-noise ratio (SNR) and evaluate the availability of each frequency during the entire campaign. The channel availability means the probability of a link to reach a minimum SNR value and hence achieve a certain quality of service as defined by *Goodman et al.* [1997]. According to *Vilella et al.* [2008], a minimum SNR value of 6 dB has been specified to estimate the channel availability in a bandwidth of 10 Hz, and this gives us compatibility to previous studies [Ads et al., 2015; Hervás et al., 2015]. The wideband sounding signal received by the receiver are used to obtain the multipath spread, the Doppler spread, the propagation time (thanks to the time accuracy of the entire system, with a time synchronization of 1 μ s) and the Doppler shift [Ads et al., 2012]. In this work, only narrowband sounding is analyzed to conduct the tests.

2.2. Vertical Incidence Sounding

The VIS parameters can be used to predict the propagation for short distance sky wave paths; in our case, applying some geometrical factors to the ionograms, the OIS properties of longer paths can be obtained [McNamara and Wilkinson, 1984]. The goal of this work is, following *Ads et al.* [2015], to compare the information about the OIS system with the VIS system analysis, in order to propose working frequencies avoiding the oblique incidence sounding and using only the VIS stations data.

As stated by *Vilella et al.* [2009], the reliability of these parameters depends on the OIS reflection point location and the distance to the closest VIS station. In Figure 1 and Table 1 several VIS stations close to the OIS path are selected to compare their measurements to the oblique sounding of the long haul link. Despite the conclusions of *Ads et al.* [2015], we have kept Port Stanley in the study, and to complete the coverage over the long haul path, we have added Sao Luis station (SAAOK), due to the lack of data of Cachoeira Paulista and Ascension Island for some campaigns.

The analysis of the VIS records focuses on the measurement of $MUF(3000)F_2$ for the purpose our study. The results of this analysis are compared to the availability of the OIS entire channel and to the estimated $MUF(D)$ by Rec533. Although the VIS stations collect data by means of different equipment (see Table 1 where we detail the type of ionosonde used in each case), all of them are Lowell Digisondes [Lowell Digisonde International, 2014], all systems use the same methodology to provide VIS data which allow us to compare results from all of them. VIS data are obtained from the Global Ionospheric Radio Observatory (GIRO) portal [Reinisch and Galkin, 2011].

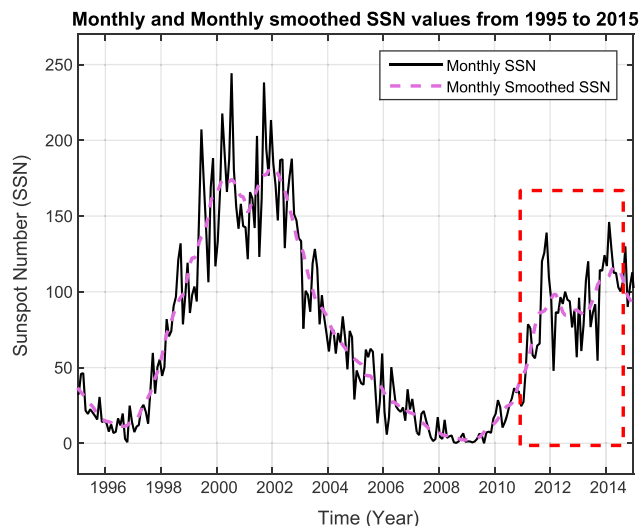


Figure 3. SSN values, with 4 month average from 1995 to 2015, remarking values of the years of our study. Values extracted from *Clette [2016]* using *Clette et al. [2014]*.

3. OIS and VIS Sounding Results Comparison

In this section we compare the OIS and the VIS sounding results for the four campaigns under study.

3.1. Heliophysical Conditions of the Experimental Study

The ionospheric propagation in HF is dependent on the solar activity together with other atmospheric circumstances. The high propagation of daytime is supported by high ionization conditions and the F_2 layer existence, but no frequencies lower than 10 MHz propagate due to the existence of the D layer [*Davies, 1990*]. The D layer complete absence during the night gives higher propagation conditions for low HF range.

A short overview of solar activity during the four surveys will give light to our analysis. Figure 3 plots an overview of the monthly smoothed sunspot number (SSN) from 1995 to 2015. In addition, the solar activity can be monitored by the solar flux; the larger the solar flux, the greater the Sun influences on ionospheric propagation. The values of the solar flux and the averaged SSN for the four campaigns are shown in Table 4, averaged for the days of activity of each campaign. The Sun is the reason for ionization of the ionosphere, so Figures 4 and 5 plot the sunrise and the sunset time for the VIS stations under study and for the estimated geographical positions for the four hops of the radio link established between the SAS and Cambrils (see Table 1 for the detail of the four hop locations). The number of hops of the radio link was studied by *Vilella et al. [2008]* based on the definitions of *Davies [1990]*. All solar activity data have been obtained from *Clette [2016]* with the method published in *Clette et al. [2014]*.

Table 4. The SSN and Solar Flux Values Measured Throughout the Four Consecutive Surveys, During the Period of the Campaign For Each Year^a

Survey	Averaged SSN	Solar Flux
2010–2011	42	89
2011–2012	56	107
2012–2013	78	116
2013–2014	123	165

^aValues extracted from *Clette [2016]* using *Clette et al. [2014]*.

Heliophysical conditions for the four surveys embrace the rising part of the solar activity cycle 24. Therefore, the four surveys cover different solar activities, from low solar activity to middle to high solar activity.

3.2. Comparison of the Evolution of the FLA and the VIS Soundings

This section compares the channel availability, the FLA measured in the receiver [*Ads et al., 2015*] obtained

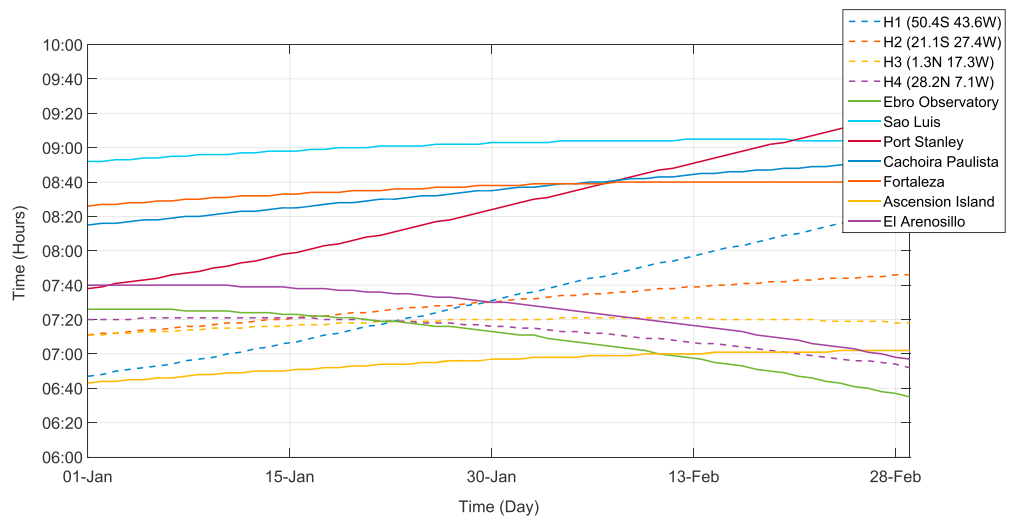


Figure 4. The sunrise time at OIS receiver, at the four reflection hops, and at the VIS stations along the path, including the range of activity days of the campaigns. For more information about the activity days in each campaign, see Table 3.

from the OIS soundings, and the VIS soundings MUF(D) predicted by Rec533 model [International Telecommunication Union-Recommendation, 2012] for the four campaigns under study.

The channel availability is the result of the narrowband study of the propagation, by means of evaluating the SNR for each hour and every frequency [Ads et al., 2015; Hervás et al., 2015] and deciding whether the propagation is good or bad comparing the SNR value with a threshold, in this case, 6 dB [Vilella et al., 2008]. This analysis has to be conducted for all the days of all campaigns, and it is presented in terms of percentage over the total days of each campaign. The FLA is selected as the frequency of highest availability for each hour of the sounding [Vilella et al., 2008].

Figure 6a clearly shows that frequencies higher than 20 MHz did not propagate properly throughout the 2010–2011 survey. The frequency of large availability (FLA) is between 4 and 10 MHz below the MUF(D); the maximum difference is around 15 UTC. No real propagation exists in frequencies higher than MUF(D).

During the 2011–2012 survey, Figure 6b, higher frequencies than 2010–2011 are achieved. The maximum frequencies able to propagate with a certain quality is 28 MHz during the daytime and 14.5 MHz during the

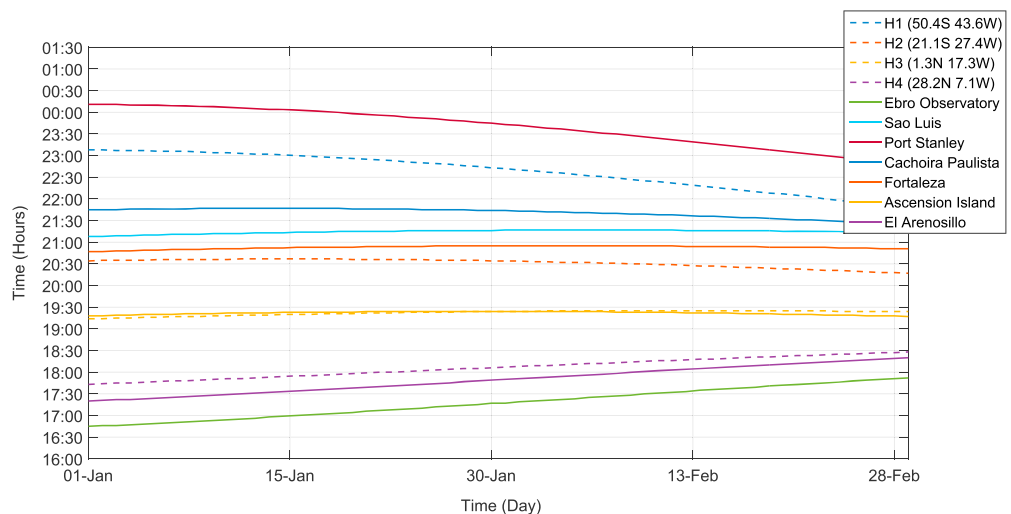


Figure 5. The sunset time at OIS receiver, at the four reflection hops, and at the VIS stations along the path, including the range of activity days of the campaigns. For more information about the activity days in each campaign, see Table 3.

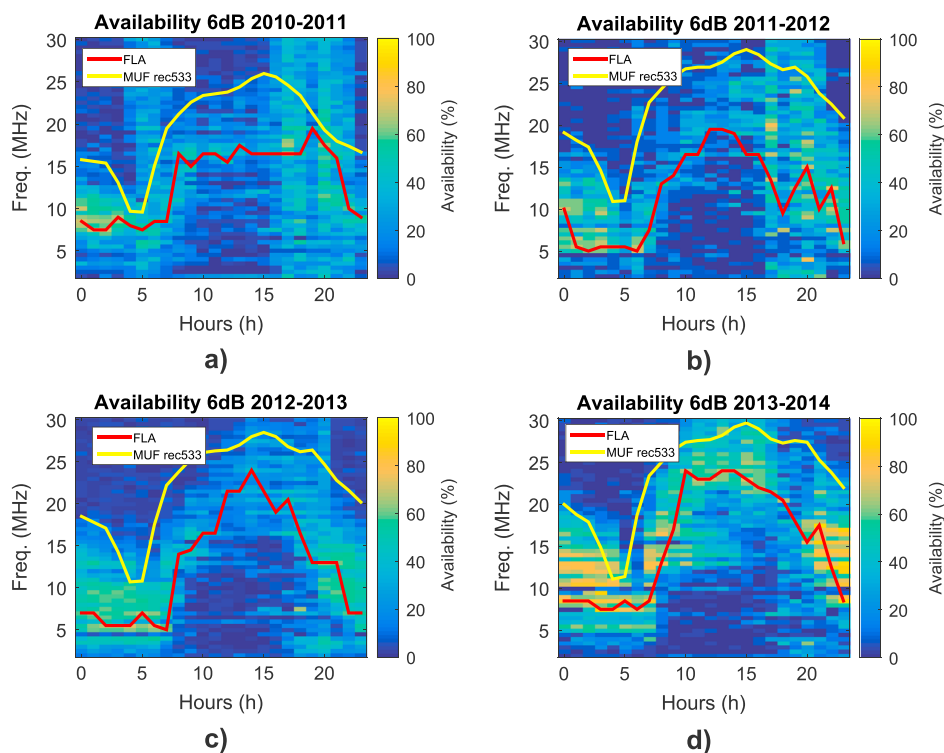


Figure 6. Comparison of interday variation (this means the data of all days in a campaign gathered to obtain the results) of FLA, MUF(D) and channel availability during (a) survey 2010–2011, (b) survey 2011–2012, (c) survey 2012–2013, and (d) survey 2013–2014.

nighttime, according to the MUF rec533 values. The FLA is about 9 MHz below the MUF(D); the maximum difference is around 18 UTC.

The 2012–2013 survey results are shown in Figure 6c. In this survey, the maximum frequencies able to be used is 27.5 MHz during the daytime and 14.5 MHz during the nighttime. The difference between FLA and MUF(D) is about 10 MHz.

Figure 6d shows the results of the 2013–2014 survey. Both MUF(D) and FLA are higher than previous surveys. The maximum frequency able to propagate properly is 30 MHz during the daytime and 19 MHz at nighttime, according to MUF rec533 values. In this survey, the difference between MUF(D) and FLA is about 6 MHz.

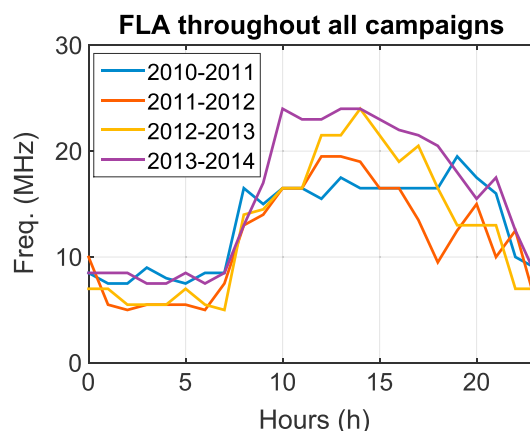


Figure 7. The FLA interday variation during 2010–2011, 2011–2012, 2012–2013, and 2013–2014 surveys.

Finally, the comparison of the FLA between these four surveys is depicted in Figure 7. The maximum frequency able to be used to propagate signal with a certain quality, higher availability values, is lower during the survey 2010–2011 than the rest of studied campaigns.

From Figure 6b and Figure 6c, we can observe that the availability of surveys 2011–2012 and 2012–2013 presents similar results. For this reason, the FLA is pretty similar. The propagated signal frequency reaches the maximum value of 19.5 MHz at 12 UTC and 24 MHz at 14 UTC, respectively. The survey 2013–2014 presents the results

Table 5. Frequencies of Maximum Channel Availability During the Four Surveys Segmented Into Daytime, Dusk, Nighttime and Dawn Regions, for an Inverted V Antenna in the Receiver in Cambrils

Survey	Daytime	Dusk	Nighttime	Dawn	Unit
	09 to 17	18 to 00	01 to 06	07 to 08	UTC
2010–2011	11 to 20	5 to 20	3.5 to 11.5	5 to 16	MHz
2011–2012	11.5 to 28	3.5 to 27.5	5 to 15.5	5 to 15	MHz
2012–2013	12.5 to 27.5	3 to 25	2.5 to 14	4 to 17.5	MHz
2013–2014	12 to 30	5 to 23	4 to 18.5	4 to 24	MHz

in terms of availability with the highest maximum frequency. For this reason, this is the campaign with the FLA of highest frequencies too.

Larger FLA for daytime compared to nighttime is expected in agreement with the daily variation of the ionospheric electron density, already described in section 3.1. We distinguish three different behaviors on the daily variations of FLA. *Nighttime* (01–06 UTC), *twilight*—which is the

transition from night to day and vice versa—(07–08 UTC corresponding to dawn and 18–00 UTC corresponding to dusk), and *daytime* (09–17 UTC). The dusk conditions stand for longer time comparing to dawn conditions, indicating the faster changes of the ionospheric transitions from night to day, when photochemical control plays a dominant role, compared to the transitions from day to night, when dynamical and electrodynamics play a role. The solar activity does not seem to play significant role for nighttime FLA, whereas daytime FLA is clearly larger for surveys with higher activity than for surveys with lower activity. A summary of these values are shown in Table 5 for the inverted V antenna; in Table 6 the results for the 7.5 m rugged monopole antenna are detailed. A summary of these values are shown in Table 5 for the inverted V antenna; in Table 6 the results for the 7.5 m rugged monopole antenna are detailed.

In *Ads et al.* [2015], the work presented uses the same transmitted data but different polarization in the receiver in Cambrils; *Ads et al.* [2015] uses a 7.5 m rugged monopole, and this work uses an inverted V. If we compare the results between *Ads et al.* [2015] and our work in campaign 2010–2011 and 2011–2012, we obtain that in campaign 2010–2011, the values of the range of frequencies of maximum availability are higher for the receptions with the monopole (which refers to vertical polarization) rather than in the inverted V antenna (which uses horizontal polarization).

This is especially clear in daytime, where the lowest frequency starts at 15 MHz for the monopole, and also at nighttime, where it starts at 7 MHz. We have to say that both in dusk and in dawn, the maximum available frequency is lower in the reception of the monopole than in the inverted V. In campaign 2011–2012 the lower bound of the range of frequencies is clearly higher for the monopole all day around, together with the fact that the upper bound of the range is clearly lower. The conclusion of the comparative study (with only two campaigns of data) is that the inverted V antenna widens the range of the frequencies of maximum channel availability in the oblique ionospheric sounding.

3.3. Vertical Incidence Sounding Results

In this section, we analyze the data recorded by the VIS stations under the study to compare them with the OIS data. This study is focused in the interday variation of the $MUF(3000)F_2$, gathering all the measured values during each ionospheric campaign. The $MUF(3000)F_2$ value corresponds to the maximum usable frequency (MUF) for a single hop transmission at 3000 km reflected at the F_2 layer, and it is extracted from the ionograms of each VIS station [*Vilella et al.*, 2009].

Table 6. Frequencies of Maximum Channel Availability During the Four Surveys Segmented Into Daytime, Dusk, Nighttime, and Dawn Regions, for a 7.5 m Rugged Monopole Antenna in the Receiver in Cambrils^a

Survey	Daytime	Dusk	Nighttime	Dawn	Unit
	09 to 17	18 to 00	01 to 06	07 to 08	UTC
2010–2011	15 to 20.5	8 to 15	7 to 9	9 to 10	MHz
2011–2012	20.5 to 25	10 to 17	6 to 11	10 to 21	MHz

^aThis information is extracted from our previous work in *Ads et al.* [2015].

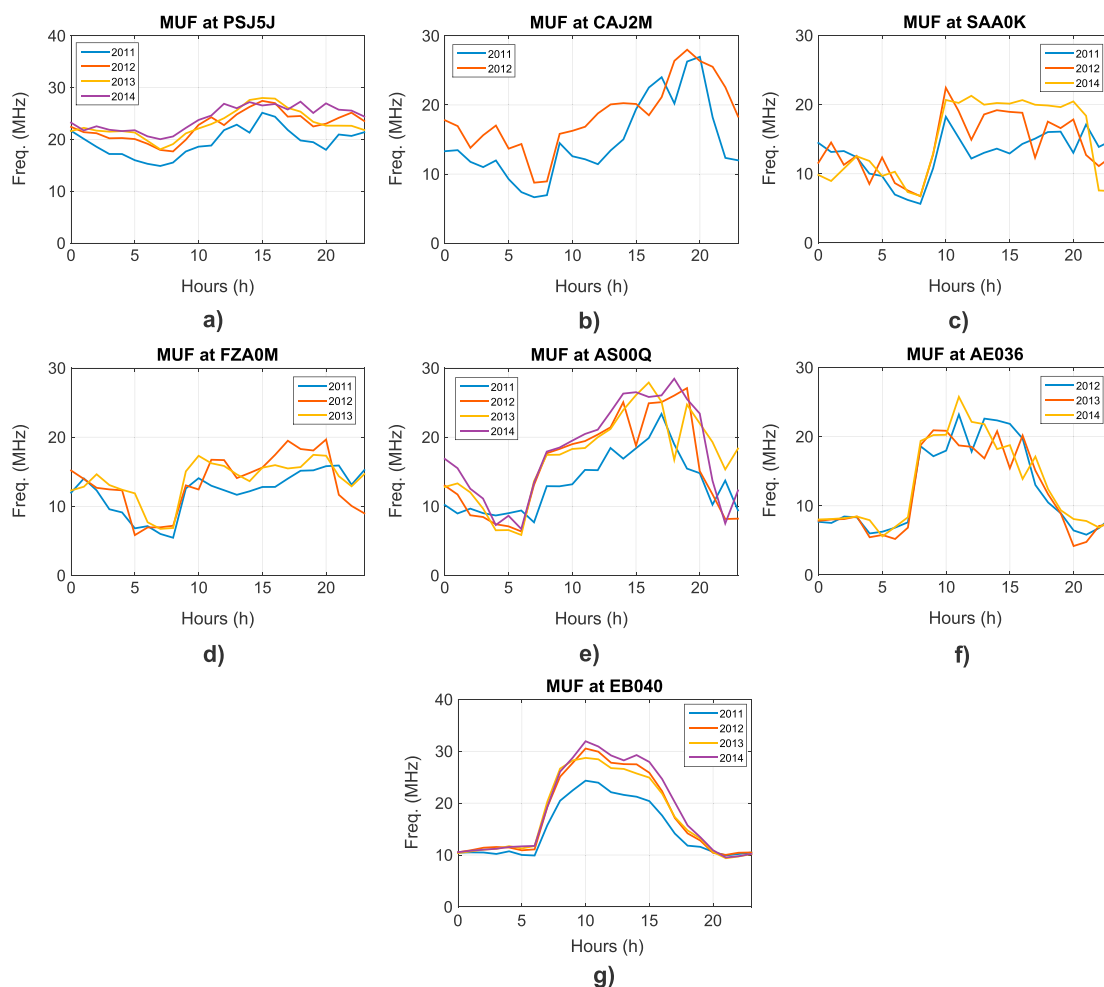


Figure 8. Interday variation of MUF(3000)F₂ during the surveys 2010–2011, 2011–2012, 2012–2013, and 2013–2014 at (a) Port Stanley station, (b) Cachoeira Paulista, (c) Sao Luis, (d) Fortaleza, (e) Ascension Island, (f) El Arenosillo, and (g) Ebro Observatory (Roquetes). Note that not all the stations have data from all the campaigns available; the availability is indicated in each figure.

Solar activity impacts on the characteristics of the different layers of the ionosphere. This has influence in the MUF(3000)F₂ which is related to latitude [Sethi *et al.*, 2002] and to solar activity history [Triskova and Chum, 1996]. For this reason, this work presents the study of the effect of the solar activity, based on the SSN value, on MUF(3000)F₂ interday variation during four consecutive surveys.

The interday variation of MUF(3000)F₂ measured by seven different VIS stations during these four surveys are shown in Figure 8. The interday variation of MUF(3000)F₂ is defined as the result of gathering the data from all the days of each campaign, and comparing these results among campaigns.

Figure 8a shows the MUF(3000)F₂ interday variation at Port Stanley station. The maximum value reaches 27.5 MHz at 15 UTC, but then, MUF(3000)F₂ decreases up to around 23 MHz during de nighttime—depending on the campaign—reaching the 20 MHz when the sunrise. Figure 8b shows data collected from Cachoeira Paulista station, which reaches the maximum MUF(3000)F₂ value at sunset (around 27 MHz), but the minimum value is found at sunrise (around 8–9 MHz). The differences observed between these two campaigns is about 2 MHz. Figure 8c shows the MUF(3000)F₂ of Sao Luis station. We can observe comparing these four surveys that the greater the SSN, the greater the MUF(3000)F₂. The maximum frequency is 22.5 MHz and is found at 10 UTC. Fortaleza (see Figure 8.d) reaches the maximum MUF(3000)F₂ value at sunset (20 UTC), with a value around 20 MHz, and the minimum values can be found between 5 and 8 UTC with around 6 MHz. Ascension station (see Figure 8e) reaches the minimum value between 4 and 6 UTC with around 7 MHz, and the maximum value at 18 UTC, around 28 MHz. Figure 8f illustrates the interday variation of MUF(3000)F₂ recorded at El Arenosillo station during the four surveys. The maximum value of 25 MHz is measured at noon time

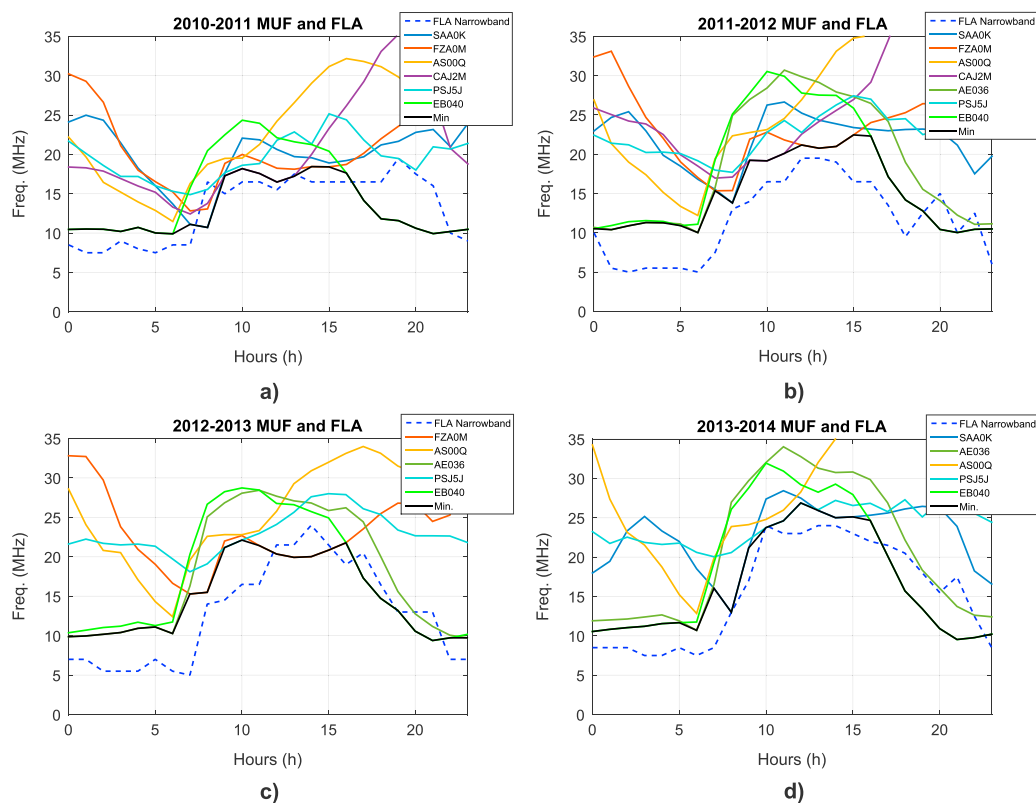


Figure 9. MUF(3000) F_2 , FLA, and the minimum MUF(3000) F_2 among the VIS stations averaged during (a) 2010–2011 survey, (b) 2011–2012 survey, (c) 2012–2013 survey, and (d) 2013–2014 survey.

(11 UTC). Finally, Figure 8g shows clearly that MUF(3000) F_2 increases during the sunrise, daytime, and sunset, for those surveys where the SSN are larger in Roquetes (Ebro Observatory station).

It is important to note in Figure 8 that all stations have both daytime and nighttime variations when comparing the different campaigns measurements. In most of them the solar activity is a key factor; when the solar activity is higher, the MUF measured is also higher. It is also clearly noticeable the higher frequencies for MUF at daytime, and the lower ones during nighttime. In this sense, campaigns 2011–2012 and 2012–2013 present similar MUF variations for nearly all stations under study for daytime and nighttime frequencies.

4. OIS and VIS Analysis Comparison

In this section we compare the MUF(3000) F_2 value recorded in each VIS station on the path of the OIS with the FLA obtained from the oblique sounding. We evaluate the minimum MUF(3000) F_2 for the long haul channel by taking the minimum MUF measurements of the VIS stations, all of them of different length, with the pretension to get the most limiting part of the ionosphere at every hour in day for each campaign.

Figure 9 illustrates the MUF(3000) F_2 recorded in all the active stations in the four campaigns under study, with the FLA of the OIS system. In order to compare the figures easily, we will divide the data into four intervals: (i) from 01 UTC to 06 UTC (nighttime), (ii) from 07 UTC to 08 UTC (twilight to dawn), (iii) from 09 UTC to 17 UTC (daytime), and (v) from 18 UTC to 00 UTC (twilight to dusk).

In the four analyzed surveys we can observe that during nighttime the FLA of the OIS is the most restrictive value represented, showing low values. The minimum value of MUF(3000) F_2 is given mostly by Ebro Observatory in this range of values in 2010–2011 campaign (when El Arenosillo is not available), and by El Arenosillo in all the other three campaigns (2011–2012, 2012–2013, and 2013–2014). In the dawn time interval the FLA presents also low values except for 2010–2011 campaign, which shows a higher value than the minimum of all the stations; in this interval, other stations like Fortaleza or Sao Luis become the propagation limits of the OIS link showing the lower MUF(3000). During daytime, the minimum values are also given by the FLA

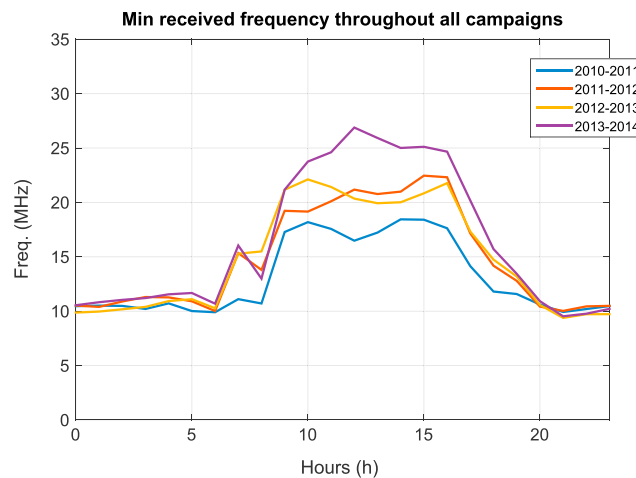


Figure 10. Minimum propagated frequency comparison throughout the 2010–2011, 2011–2012, 2012–2012, and 2013–2014 surveys, from the data of the $MUF(3000)F_2$ of the analyzed VIS stations.

in the OIS sounding, but the minimum value of $MUF(3000)F_2$ is closer to the FLA result. The limiting values are given by Fortaleza and Cachoeira Paulista in 2010–2011 and 2011–2012 campaigns (when both station data are available), by Fortaleza in 2012–2013 campaign (where nor Cachoeira Paulista or Sao Luis data were available), and finally, by Sao Luis and Port Stanley in 2013–2014 campaign (where nor Cachoeira Paulista or Fortaleza data were available). Finally, in dusk time interval the minimum of the stations, mostly defined by El Arenosillo (and Ebro Observatory when the previous is not available), present lower values than the FLA for several hours.

To sum up, from Figure 9 it is clearly evident that the combination of the minimum MUF daily variation compares and correlates pretty well with the day variation of FLA for all the surveys. Exception to this is for survey 2010–2011 at dusk, where FLA is larger than the minimum MUF. To evaluate numerically this conclusion, we have calculated the correlation coefficient between the minimum value of MUF for all stations (in the figures “Min”) and the FLA of the narrowband study. The correlation coefficient for 2010–2011 campaign is 0.61, while the *R* value for 2011–2012 campaign is 0.82. Campaign 2012–2013 shows a correlation coefficient of 0.82, and finally, campaign 2013–2014 *R* value is 0.85. The similitude between the pair array values is high enough to conclude that the two magnitudes present a correlation.

Finally, in Figure 10, the minimum of $MUF(3000)F_2$ evolution in the four studied surveys is shown. The night-time time range show similar results in terms of minimum frequency for the three campaigns that have used El Arenosillo in the comparison (2011–2012, 2012–2013, and 2013–2014); 2010–2011 campaign presents similar values given by Ebro Observatory, especially close to midnight. The same happens for the dusk time interval, where the three last campaigns present similar values. During dawn and daytime, the minimum values are higher in frequency, being 2010–2011 campaign the lowest of the minimums. These results are related to the SSN and solar flux unit (SFU) values detailed in Table 4; the minimum values correspond to 2010–2011 campaign, and the maximum ones—strictly related to the propagation—correspond to campaign 2013–2014, where we achieve the best results in terms of availability and frequency. In this sense, we can conclude that campaigns 2011–2012 and 2012–2013 present similar values of propagated frequency, as it already happened in Figure 8 for the MUF detailed in all the stations under study.

5. Conclusions

The aim of this work was to conclude the validation of the prediction method for the best frequency transmissions of a long haul 12,760 km channel transequatorial link between Livingston and Spain without the oblique sounding data. This study is the continuation of the work published by *Ads et al.* [2015], where a first proof of concept was developed; in this paper the validation is conducted using a different antenna in the receiver (an inverted V instead of a 7.5 m rugged monopole), we have changed slightly the location of the receiver and we have increased the number of campaigns studied from 3 to 4 (half of them different from the ones studied previously).

An oblique sounding of the channel was performed, with a 7.5 m rugged monopole in the transmitter in Livingston and an inverted V antenna in the receiver in Cambrils, and its results have been compared to the results of the six VIS stations along the path. The comparison between $MUF(3000)F_2$ obtained by the VIS stations and FLA obtained by the oblique sounding confirms us a good results in terms of prediction: in the four analyzed campaigns, there is clear dependency between the minimum $MUF(3000)F_2$ obtained by the VIS stations and the FLA computed by the oblique sounding. Despite that the VIS stations are not equally separated from the path, we conclude that twilight and nighttime are governed by the ionospheric conditions close to the last hop before reception, which in this study coincides with El Arenosillo station (or Ebro Observatory when El Arenosillo is not available). Whereas for daytime conditions, the ionospheric conditions observed at the near equator stations seem to limit the transmission conditions.

The minimum propagated frequency during the daytime is increased by around 1 h from the first to the last survey. This is highly related to the increasing of the SSN and solar flux from 24 (2010–2011) to 91 (2013–2014) and from 89 to 165 SFU, respectively. Thus, the solar activity period seems to play a significant role for OIS, although nighttime FLA seems to be insensitive to different solar activity levels observed for different surveys, the daytime FLA is clearly larger for surveys with higher activity than for surveys with lower activity. Similarly, the solar activity is a key factor for VIS; when the solar activity is higher, the MUF measured is also higher. It is also clearly noticeable the higher frequencies for MUF at daytime, and the lower ones during nighttime. In this sense, campaigns 2011–2012 and 2012–2013 present similar MUF results for nearly all stations under study.

Moreover, we have corroborated that the lowest $MUF(3000)F_2$ recorded at the VIS stations located strategically close to the link is similar to the FLA values at a given time. Thus, using the information of the measurements furnished by VIS located along the radio path can serve to predict the FLA of this transequatorial radio link.

Another important outcome of this study is that the use of inverted V antenna at the receiver site widens the range of the frequencies of maximum channel availability in the oblique ionospheric sounding compared to the range of frequencies we receive while using the rugged monopole, i.e., it widens the range of the frequencies that can be used for the radio transmission. This indicates also that the horizontal polarization, received by the inverted V antenna, suffers less attenuation than the vertical polarization, received by the rugged monopole. This is based on the results of two surveys with simultaneous reception of different polarizations and might be the result of low elevation angle of the signal at the receiver, making more effective the reception of the horizontal polarization compared to the vertical polarization.

Notation

- ADC analog to digital converter.
- AS00Q Ascension Island Station.
- CB Cambrils.
- CAJ2M Cachoeira Paulista Station.
- DAC digital to analog converter.
- EA036 El Arenosillo Station.
- EB040 Roquetes-Ebro Observatory.
- FLA frequency of large availability.
- FZA0M Fortaleza Station.
- HF high frequency.
- ITU International Telecommunication Union.
- MUF maximum usable frequency.
- OCXO oven controlled crystal oscillator.
- OIS oblique incidence Sounder.
- P5J5J Port Stanley Station.
- SAA0K San Luis Station.
- SAS Spanish Antarctic Station.
- SDR software-defined radio.
- SF solar flux.
- SSN sunspot number.
- VIS vertical incidence sounding.
- UTC coordinated universal time.

Acknowledgments

This work has been funded by the Spanish Government under the projects CGL2006-12437-C02, CTM2008-03536-E, CTM2009-13843-C02, CTM2010-21312-C03, and CTM2014-52182-C3-1-P. Rosa Ma Alsina Pagès and Marcos Hervás thank the Secretaria d'Universitats i Recerca del Departament d'Economia i Coneixement (Generalitat de Catalunya), under grant 2014-SGR-0590 and 2015-URL-Proj-046, for funding partially the study that led to this paper. David Altadill and Estefania Blanch were supported by Universitat Ramon Llull projects 2016-URL-Trac-001 and 2016-URL-Internac-027 funded by Obra Social la Caixa and 2016-URL-IR-001 funded by Generalitat de Catalunya. We also acknowledge the Global Ionospheric Radio Observatory (GIRO) and GIRO Principal Investigator B. W. Reinisch of the University of Massachusetts Lowell and GIRO data providers for making data available. Long haul ionospheric Antarctic link data are available at IGME (Instituto Geológico y Minero de España) after registration.

References

- Ads, A. G., P. Bergadà, C. Vilella, J. R. Regué, J. L. Pijoan, R. Bardaji, and J. Mauricio (2012), A comprehensive sounding of the ionospheric HF radio link from Antarctica to Spain, *Radio Sci.*, *48*, 1–12, doi:10.1029/2012RS005074.
- Ads, A. G., P. Bergadà, J. R. Regué, R. M. Alsina-Pagès, J. L. Pijoan, D. Altadill, D. Badia, and S. Graells (2015), Vertical and oblique ionospheric soundings over the long haul HF link between Antarctica and Spain, *Radio Sci.*, *50*, 916–930, doi:10.1002/2015RS005773.
- Alsina-Pagès, R. M., M. Hervás, F. Orga, J. L. Pijoan, D. Badia, and D. Altadill (2016), Physical layer definition for a long haul HF Antarctica to Spain radio link, *Remote Sens.*, *8*(5), 380.
- Angling, M. J., P. S. Cannon, N. C. Davies, T. J. Willink, V. Jodalen, and B. Lundborg (1998), Measurements of Doppler and multipath spread on oblique high latitude HF paths and their use in characterizing data modem performance, *Radio Sci.*, *33*(1), 97–107.
- Bergadà, P., R. M. Alsina-Pagès, and M. Hervás (2016), Polarization diversity in a long-haul transequatorial HF link from Antarctica to Spain, *Radio Sci.*, *52*, 105–117, doi:10.1002/2016RS006136.
- Davies, K. (1990), *Ionospheric Radio*, Peter Peregrinus, London, U. K.
- Clette, F. (2016), *Sunspot Index and Long-Term Solar Observations*, Royal Observatory of Belgium Av. Circulaire, Brussels, Belgium. [Available at <http://www.sidc.be/silso/home>, (last accessed 5th Dec 2016).]
- Clette, F., L. Svalgaard, J. M. Vaquero, and E. W. Cliver (2014), Revisiting the sunspot number. A 400-year perspective on the solar cycle, *Space Sci Rev.*, *186*, 35–103, doi:10.1007/s11214-014-0074-2.
- Gold, R. (1968), Maximal recursive sequences with 3-valued recursive cross-correlation functions, *IEEE Trans. Inf. Theory*, *14*(1), 154–156.
- Goodman, J., J. Ballard, and E. Sharp (1997), A long-term investigation of the HF communication channel over middle- and high-latitudes paths, *Radio Sci.*, *32*(4), 1705–1715.
- Hervás, M., R. M. Alsina-Pagès, F. Orga, D. Altadill, J. L. Pijoan, and D. Badia (2015), Narrowband and wideband channel sounding of an Antarctica to Spain ionospheric radio link, *Remote Sens.*, *7*(9), 11,712–11,730.
- International Telecommunication Union-Recommendation (2012), Method for the prediction of the performance of HF circuits, *Recomm. P533-11*, ITU, Geneva, Switzerland.
- Jackson-Booth, N. K., P. S. Cannon, M. M. Bradley, and P. A. Arthur (2012), New oblique sounders for ionospheric research, paper presented at 12th IET International Conference on Ionospheric Radio Systems and Techniques (IRST 2012), York, U. K., 15–17 May.
- Jodalen, V., T. Bergsvik, P. S. Cannon, and P. C. Arthur (2001), Performance of HF modems on high-latitude paths using multiple frequencies, *Radio Sci.*, *36*(6), 1687–1698.
- Lowell Digisonde International, Inc. (2014). Digisonde Station List. [Available at <http://digisonde.com/stationlist.html>, (last accessed 2017-04-13).]
- McNamara, L., and P. Wilkinson (1984), A cautionary note on the use of F2 layer correlation coefficients for short-term forecasting purposes, paper presented at 1984 Solar-Terrestrial Predictions: Proceedings of a Workshop at Meudon, Meudon, France, Jun.
- Perkiomaki, J. (2013), HF propagation prediction and ionospheric communications analysis—VOACAP. [Available at www.voacap.com.]
- Parsons, J. D. (2000), *Mobile Radio Propagation Channel*, John Wiley, New York.
- Pijoan, J. L., D. Altadill, J. M. Torta, R. M. Alsina-Pagès, S. Marsal, and D. Badia (2014), Remote geophysical observatory in Antarctica with HF data transmission: A review, *Remote Sens.*, *6*(8), 7233–7259, doi:10.3390/rs6087233.
- Proakis, J. (2000), *Digital Communications*, McGraw Hill, New York.
- Reinisch, B. W., and I. A. Galkin (2011), Global Ionospheric Radio Observatory (GIRO), *Earth Planets Space*, *63*, 377–381, doi:10.5047/eps.2011.03.001.
- Sethi, N. K., M. K. Goel, and K. K. Mahajan (2002), Solar cycle variations of foF2 from IGY to 1990, *Ann. Geophys.*, *20*(10), 1677–1685, doi:10.5194/angeo-20-1677-2002.
- Shukla, A. K., and P. S. Cannon (1994), Prediction model updating using the ROSE-200 oblique ionospheric sounder at mid and higher latitudes, paper presented at 6th International Conference on HF Radio Systems and Techniques, IET, York, U. K., 4–7 Jul.
- Triskova, L., and J. Chum (1996), Hysteresis in dependence of foF2 on Solar indices, *Adv. Space Res.*, *18*(6), 145–148.
- Vilella, C., D. Miralles, and J. L. Pijoan (2008), An Antarctica-to-Spain HF ionospheric radio link: Sounding results, *Radio Sci.*, *43*, RS4008, doi:10.1029/2007RS003812.
- Vilella, C., D. Miralles, D. Altadill, F. Acosta, J. G. Solé, J. M. Torta, and J. L. Pijoan (2009), Vertical and oblique ionospheric soundings over a very long multihop HF Radio link from polar to midlatitudes: Results and relationship, *Radio Sci.*, *44*, RS2014, doi:10.1029/2008RS004001.
- Warrington, E. M., C. A. Jackson, A. J. Stocker, T. B. Jones, and B. Lundborg (2000), Observations of the directional characteristics of obliquely propagating HF radio signals and simultaneous HF radar measurements, *IEEE Conf. Publ.*, *474*, 243–267.